# Sparse estimation based monitoring method for damage detection and localization: A case of study

Mahjoub El Mountassir, Slah Yaacoubi, Gilles Mourot, Didier Maquin

# Sparse estimation based monitoring method for damage detection and localization: A case of study

**Mahjoub El Mountassir[1,2], Slah Yaacoubi[1], Gilles Mourot[2], Didier Maquin[2]**

[1]Institut de soudure, Plateforme RDI CND, 4 Bvd Henri Becquerel

57970 Yutz France (m.elmountassir, s.yaacoubi)@isgroupe.com

[2]Centre de Recherche en Automatique de Nancy, CNRS, Université de Lorraine,

2 Avenue de la Forêt de Haye, TSA 60604, 54 518 Vandoeuvre-lès-Nancy, France

(gilles.mourot, didier.maquin)@univ-lorraine.fr

---

Abstract: This paper suggests a Structural Health Monitoring (SHM) method for damage detection and localization in pipeline. The baseline signals, used in SHM, could change due to the variation of environmental and operational conditions (EOCs). Hence, the damage detection method could give rise to false alarm. In this study, this issue is addressed by estimating the current signal using only few reference signals with similar or very close EOCs. Such an operation can be performed by calculating a sparse estimation of the current signal. The estimation error is used as an indication of the presence of damage. Actually, a signal from the damaged pipe will be characterized by a high estimation error compared to that of a signal from the undamaged pipe. The damage location is obtained by calculating the estimation error on a sliding window over the signal from the damaged pipe. This method was tested on signals collected on a 6 m pipeline segment placed in a workshop under natural temperature variations. Results have shown that the created damage was successfully detected and localized.

*Keywords:* Structural Health Monitoring, sparse estimation, damage detection, damage localization, environmental and operational conditions.

---

## 1. INTRODUCTION

Structural Health Monitoring (SHM) techniques are intended to assess the integrity of structures, such as pipelines [1–3]. They are developed in order to avoid failures, which could occur as consequence of a critical damage. Some failures might give rise to considerable material, human and institutional losses. The damage could have different types and forms, where the most faced one is corrosion because of the huge use of carbon steel pipelines. SHM techniques aim at detecting the initiation of damage (i.e. at early stages) to perform thereafter the maintenance of the damaged area of the structure, without any delay. Technically speaking, early stages defect detection is ensured thanks to the monitoring, which is somewhat based on the comparison between the reference signals (i.e. baseline) obtained from the healthy structure and the current one (i.e. the structure can be damaged or still healthy). Regarding the monitoring of pipelines integrity, the signals are acquired using ultrasonic guided waves (UGW) technique [4]. UGW can travel over long distances with relatively small attenuation [5]. Hence, they can cover large areas using only small numbers of distributed sensors. These waves interact with the structures heterogeneity such as weld, flange, defect etc.

The task of comparison between the reference signal and the current signal is not easy to achieve because the healthy state of the structure could vary due to the changes in the environmental and operational conditions (EOCs) (e.g. temperature, humidity, vibration loads, etc.) [6]. The effects of these EOCs could be similar to those produced by damage [7,8]. This would result in false warnings. The differentiation between the aforementioned types of changes is a challenging task. In the literature, different approaches were proposed to address this issue. They can be classified into two categories: analytical and statistical methods. Clarke et al [9] have proposed to combine two analytical methods (optimal stretch method and optimal baseline method) to compensate the effect of temperature on guided wave propagation. The first method is applied when temperature effect is

dilation/compression of the received signal. However, some experimental works have demonstrated that temperature effect is not only a change of the propagation time but also a significant change in the amplitude of the signals [10,11]. The second method requires a database of reference signals acquired at different temperatures. Each time a new current signal is presented, it selects from the database of reference signals the one that gives a lower subtraction error. But, the reliability of this method depends on the temperature gap between the baselines which should be very small. This implies a huge database of reference signals. Furthermore, damage detection with these methods is based on a simple subtraction between the reference signal and current signal, which is not reliable. Concerning statistical methods, Rizzo et al [12] applied novelty detection for defect detection in railroad using UGW. They have proposed to build a database of reference signals by adding a random noise to a baseline signal acquired from an undamaged mock up railroad. However, the added noise cannot be used to simulate the effects of EOCs. A more realistic study was developed by Chang et al [13], they have proposed an unsupervised damage detection method using Singular Value Decomposition (SVD) of the matrix of collected signals. It was developed on the premise that the effect of damage and the effect of EOCs will be represented in different singular vectors. In this case, damage is detected by observing a jump of the mean in the right singular vectors. But the question here is in which singular vector the jump can be observed and how can we automatically detect this jump. Also, this can be only done in the case where the following hypotheses are fulfilled. Firstly, it supposes that damage occurs abruptly, which is not always true because in real cases, damage may develop progressively during a long period of time. Secondly, EOCs should be constantly changing so a jump cannot be observed in their associated singular vectors, otherwise it will be considered as an indication of the presence of damage. Here also temperature changes for example could have a clear trend, so in this case the latter hypothesis might be not verified. More recently, Eybpoosh et al [14] have proposed a supervised method based on sparse representation of UGW signals, which can ensure discrimination between damage and

variation in EOCs. However, this method requires the use of signals from the damaged pipe, which are generally not available. Indeed, in real world, when damage occurs, it progresses arbitrary. That is to say, a database collected in a given structure could not be used for others. Consequently, the aforementioned method may not be reliable in industrial context.

In this study, since signals from the undamaged pipe are the only available information which can be provided in the training step, the proposed method for damage detection is based on a novelty detection technique. To deal with variation in EOCs, we consider a method of learning in non-stationary environment. This method consists in estimating the current signal by only few signals among the reference database. Physically, if the current signal is from a healthy pipe, it will be estimated using few reference signals with similar or very close EOCs, the others being discarded. As all identification methods, the proposed approach is based on the assumption that the database of reference signal contains sufficient variation of EOCs. Otherwise, an update of the reference database is necessary to ensure viable damage detection. Such development is not implemented in the present study. Note here that the difference between the proposed method and the optimal baseline selection method is that the latter searches for only one baseline signal that matches the current signal in terms of temperature variation. While the proposed approach searches for a combination of reference signals that well estimate the current signal. The estimated signal is obtained by averaging the found reference signals with a specific weight for each one. To localize the damage, we suggest applying the sparse estimation on a sliding window over the signal from the damaged pipe. This is motivated by the fact that when dealing with UGW the effect of damage is local on the signal.

In the next section, the proposed methodology for damage detection and localization in pipeline is presented. In section 3, the procedure for collecting the database of signals from the healthy pipe and the damaged pipe is explained. Also, the pre-processing of these signals is exposed. Section 4 is devoted to discussions on the obtained results. Finally, section 5 concludes the paper.

## 2. MATHEMATICAL BACKGROUND AND PROBLEM FORMULATION

### 2.1 Overview of the sparsity problem

The monitoring process of a structure begins generally by collecting reference signals at different EOCs during a fixed period of time. Afterthat, whenever a new current signal is presented, it must be compared to these reference signals. In this paper, the proposed approach for comparing the current signal to the reference signals consists in first estimating the current signal by only a few reference signals as shown in Figure 1. Then, we calculate the estimation error which will be used to construct a damage index. The question here is how to select from the database of reference signals those which will be used to estimate the current signal. This could be done by feature selection techniques used in machine learning. However, the problem is not only to select the suitable reference signals but also to search for the fewest number of them. Such an issue is commonly known as sparsity problem. The next section is devoted to describe the methodology that has been followed to estimate a new current signal.

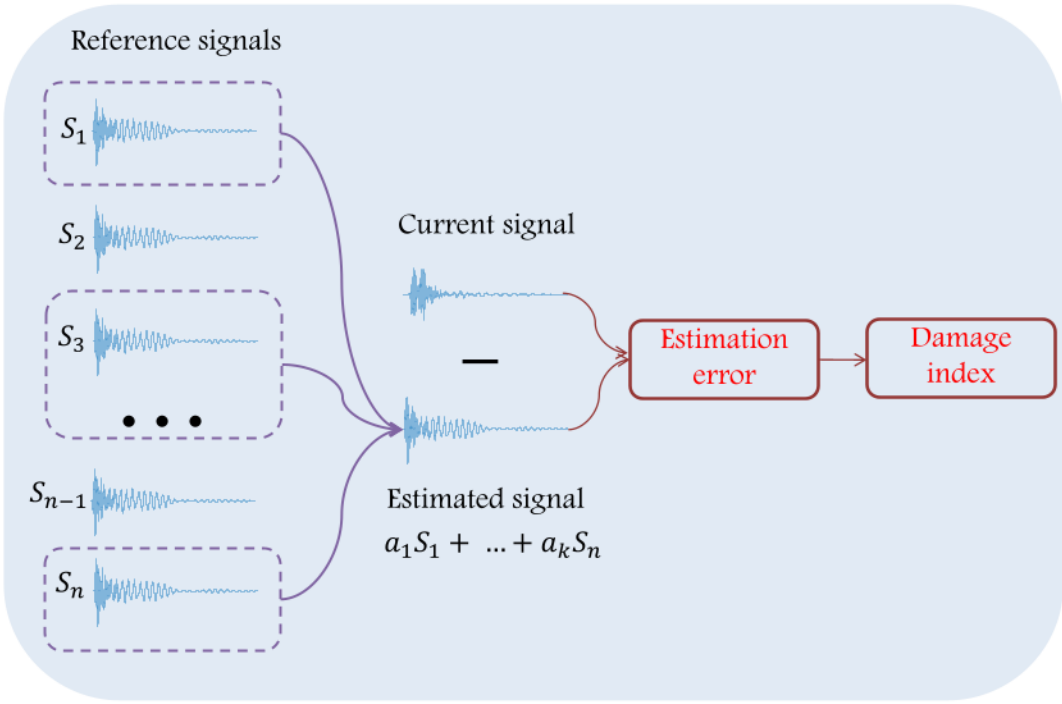


**Figure 1.** Overview of the sparsity approach used for damage detection in pipeline

### 2.2 Sparse estimation

Initially, an estimation of the current signal $\boldsymbol{x} \in \mathbb{R}^m$ by the matrix of reference signals $C \in \mathbb{R}^{m \times n}$ could be provided by minimizing the quadratic error given below:

$$\mathrm{J}(\boldsymbol{\theta}) = \|C\boldsymbol{\theta} - \boldsymbol{x}\|_2^2 \qquad (1)$$

$$\widehat{\boldsymbol{\theta}} = \arg\min_{\boldsymbol{\theta}} \mathrm{J}(\boldsymbol{\theta}) \qquad (2)$$

where $\boldsymbol{\theta} \in \mathbb{R}^n$ is the vector of regression coefficients, $m$ and $n$ are the number of samples and the number of reference signals respectively.

The optimal regression coefficients $\widehat{\boldsymbol{\theta}}$ provide an estimation of the current signal using all the reference signals. But, the current signal is measured in specific EOCs while the reference signals are generally acquired in a wide range of EOCs. Hence, such estimation could give rise to an overfitting. This will jeopardize damage detectability because the regression model will tend to minimize the estimation error for a signal from the damaged pipe, which should be very high compared to that of a reference signal. Besides, the coefficients should be positive to avoid the compensation between the reference signals. To overcome this issue, sparsity on the regression coefficients must be defined. It can be obtained by adding a regularisation term to equation (2) as following:

$$\widehat{\boldsymbol{\theta}} = \arg\min_{\boldsymbol{\theta}} \left(\mathrm{J}(\boldsymbol{\theta}) + \lambda \|\boldsymbol{\theta}\|_1\right) \qquad (3)$$

$$\text{subject to } \boldsymbol{\theta} \geq \mathbf{0}$$

This optimization problem can be solved using the lasso method with non-negative constraint [15]. The optimal solution will select from the reference signals a subset, which will be used to estimate the current signal and assign zero to the others. The tuning parameter $\lambda$ controls the power of regularization and it must be chosen in the training step. Generally, it is very difficult to determine a value of this parameter. It requires the use of cross validation technique. In this context, some studies have shown that in the case of positively correlated signals, non-negative least square (NNLS) is an efficient regularization technique [16,17]. In other words, we can say that the method

has a self-regularization property, which means that it can automatically generate a regularization term. Thus, there is no need to determine the tuning parameter λ. The condition of positively correlated variable is generally true for UGW signals (this will be verified in section 4.1). This condition is fulfilled if all the entries of the covariance matrix $S$ of $C$ are strictly positive. Mathematically, it can be expressed as:

$$\min_{i,j}\big(S\,(i,j)\big) \geq \sigma > 0 \qquad (4)$$

where $S = \frac{1}{n} C^T C$ and $\sigma$, a strictly positive scalar.

It is worth noting here that the farther the parameter σ is to zero, the higher the self-regularizing effect.

The NNLS problem is defined as:

$$\widehat{\boldsymbol{\theta}} = \arg\min_{\boldsymbol{\theta}} \mathrm{J}(\boldsymbol{\theta}) \qquad (5)$$

$$\text{subject to } \boldsymbol{\theta} \geq 0$$

To get an optimal solution of this problem, the Karush-Kuhn-Tucker (KKT) conditions must be satisfied. These conditions are defined as follows [18]:

$$\widehat{\boldsymbol{\theta}} \geq 0 \qquad (6)$$

$$\nabla \mathrm{J}\big(\widehat{\boldsymbol{\theta}}\big) \geq 0 \qquad (7)$$

$$\nabla \mathrm{J}\big(\widehat{\boldsymbol{\theta}}\big)^T \widehat{\boldsymbol{\theta}} = 0 \qquad (8)$$

where ∇J denotes the gradient. Its expression is given by:

$$\nabla \mathrm{J}\big(\widehat{\boldsymbol{\theta}}\big) = 2C^T\big(C\widehat{\boldsymbol{\theta}} - \boldsymbol{x}\big) \qquad (9)$$

The constrained minimization problem described in equation (5) can be solved using different numerical approaches. The most common ones are: active set method, projected quasi Newton approach, principal block pivoting method and interior point method [19]. A comparison between these approaches is beyond the scope of this study. However, we have chosen to use the active set method because a recursive version of this method can be easily implemented. This will be used

later for the purpose of damage localization. Active set method divides the constraints into active and passive ones. Actually, the active constraint refers to zero regression coefficients, otherwise it is considered as passive. At each step, the method calculates the solution by the least squares method on the passive set. Then, it tests if the new regression coefficients satisfy the KKT conditions. Afterthat, it updates the set of active coefficients until a final set is found. Lawson and Hanson [20] have proposed an algorithm to solve NNLS problem, which is an active set method. It is described in the following flowchart.

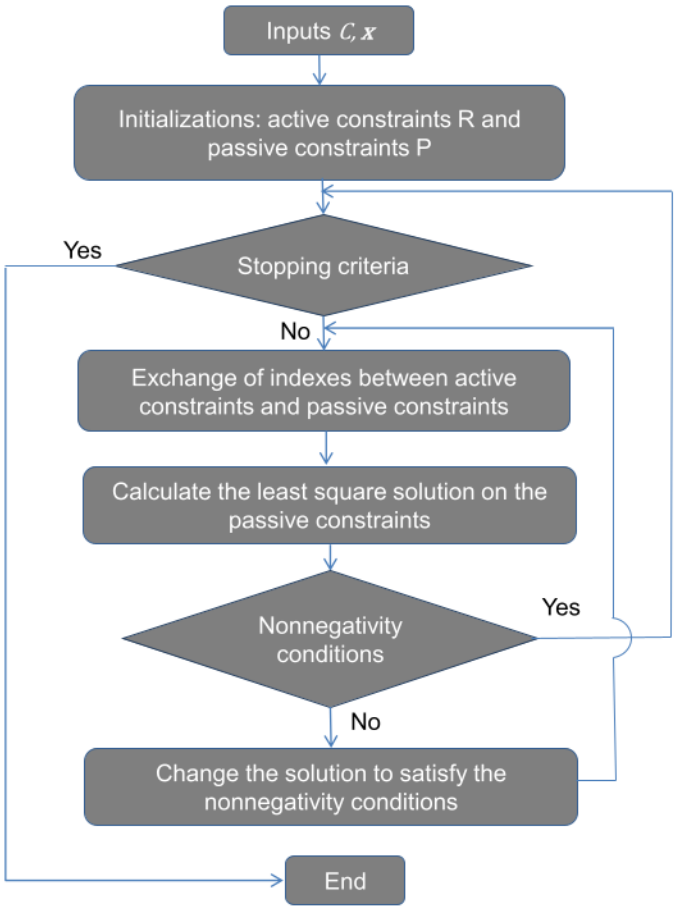


**Figure 2**. Algorithm used for solving a non-negative least square problem

### 2.3 Damage indicators

To detect the presence of damage, an indicator must be derived from the sparse estimation of the current signal. If the signal is from a damaged structure, we expect that the estimation error will be

very high compared to that of a reference signal. Hence, a damage indicator could be chosen as the quadratic estimation error $\mathrm{J}(\widehat{\boldsymbol{\theta}})$ given by the solution of NNLS problem described in equation (5).

The sparsity of the regression coefficients ($Sr$) could be also used as damage indicator [21]. It is defined as the ratio of the number of zero coefficients in $\widehat{\boldsymbol{\theta}}$ to the total number of reference signals:

$$Sr = \frac{n - \mathrm{card}(P)}{n} \times 100 \qquad (10)$$

where $\mathrm{card}(P)$ denotes the cardinal of the final set of the passive constraints $P$. In fact, a signal from the damaged pipe will be characterized by a very small number of passive coefficients. Hence, the value of $Sr$ will converge to unity. While, for a reference signal, the value of $Sr$ will be theoretically a little far from unity. Furthermore, this sparsity will increases as the damage size increases. Thus, the damage severity can be assessed using this factor.

A joint damage indicator $I$ that account for both the quadratic estimation error and the sparsity ratio could be established to maximize the chances for damage detectability as proposed in [22]. It is defined by the vector:

$$I = (\mathrm{J}(\widehat{\boldsymbol{\theta}}), Sr) \qquad (11)$$

To ensure automatic damage detection, a threshold must be defined. For this purpose, in the case of one dimensional damage indicator (i.e. $\mathrm{J}(\widehat{\boldsymbol{\theta}})$ or $Sr$), an empirical distribution for damage indicators, calculated from reference signals, has to be established. Afterthat, the threshold can be chosen by fixing the confidence limit of the distribution. The current signal is considered as damage if its damage indicator exceeds the value of the specified confidence limit.(  ) The procedure of damage detection in this case is shown in Figure 3. When using a bivariate indicator as defined in equation (11), the signals will be represented in a two-dimensional space. In this case, the threshold can be chosen by defining a metric to measure how close the damage indicator vector of the current signal to those of the reference signals. This metric can be calculated using multivariate statistical tools such as the Mahalanobis Square Distance [23].

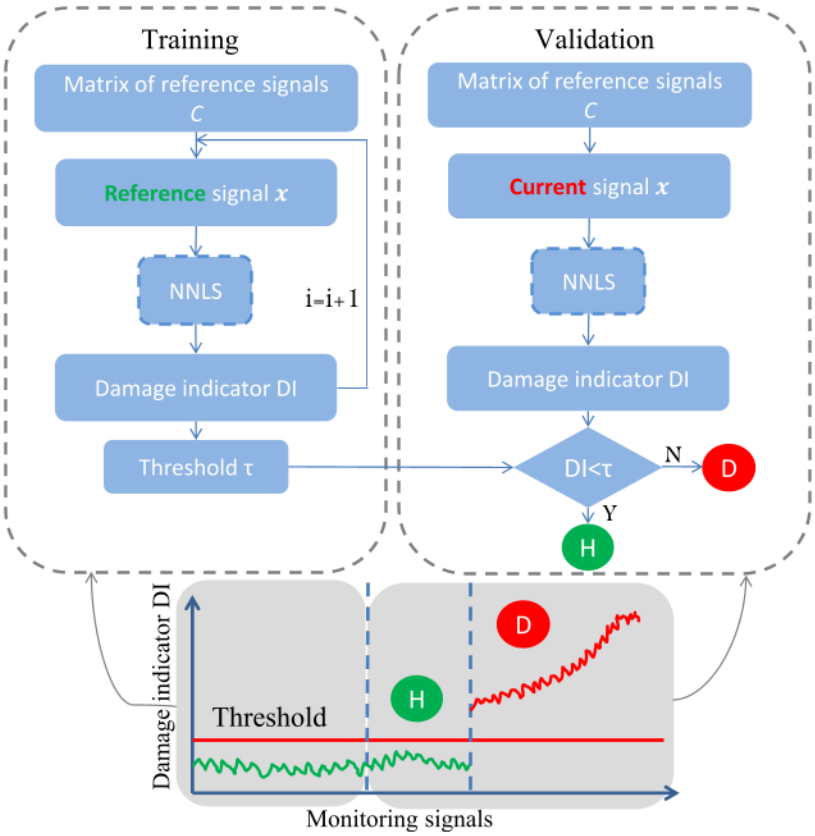


**Figure 3.** Proposed damage detection procedure, where H and D denote healthy and damaged states of the pipe, respectively, i, an integer.

### 2.4 Damage localization using recursive NNLS

To get the position of damage, we suggest calculating the sparse estimation of the signal from the damaged pipe on a sliding window over the matrix of reference signals. The already found regression coefficients, obtained for the entire signal, are no longer suitable. Hence, the solution of NNLS problem must be obtained for every sliding window. Taking into consideration the fact that adding and removing one sample at a time do not change significantly the regression coefficients found in the previous window, it is of interest to apply a recursive version for the solution of the NNLS.

In the case of classical least squares method (unconstrained), a method to update the regression coefficients already exists [24]. It is known as Recursive Least Squares (RLS). Since the NNLS solving method requires the use of least squares on the passive set, the RLS could be applied to

update NNLS solution. However, the non-negativity of the new regression coefficients is not guaranteed. In other words, the KKT conditions could be violated. Thus, to get an optimal solution of the recursive NNLS problem, these KKT conditions must be verified. Afterthat, a pivoting exchange between the passive set and the active set could be eventually needed [25]. Under the assumption of minimal set changes, we expect that only a single pivoting exchange is made between the active set and the passive set. Hence, block pivoting is not necessary in this case.

The calculation of the RLS on a sliding window includes two successive steps: updating and downdating [26]. The former adds a new sample to the window and the latter removes a sample, which is excluded from the sliding window. Let us denotes by $H$ the window width and by $k$ the index of the sample. The algorithm starts first with a window which comprises samples from $k$ to $k+H-1$. This window corresponds to the matrix of reference signals $C_{k+H-1}$ and the current signal $\boldsymbol{x}_{k+H-1}$. The solution in this case is denoted as $\widehat{\boldsymbol{\theta}}_{k+H-1}$.When adding a new sample $(\boldsymbol{c}_{k+H}, x_{k+H})$ where $C_{k+H} = \begin{pmatrix} C_{k+H-1} \\ \boldsymbol{c}_{k+H} \end{pmatrix}$ and $\boldsymbol{x}_{k+H} = \begin{pmatrix} \boldsymbol{x}_{k+H-1} \\ x_{k+H} \end{pmatrix}$, the updating operation can be written as:

$$A_{k+H-1} = (C_{k+H-1}^T C_{k+H-1})^{-1} \tag{12}$$

$$\boldsymbol{\beta}_{k+H} = \frac{A_{k+H-1}\boldsymbol{c}_{k+H}^{\boldsymbol{T}}}{1 + \boldsymbol{c}_{k+H} A_{k+H-1} \boldsymbol{c}_{k+H}^{\boldsymbol{T}}} \tag{13}$$

$$\widehat{\boldsymbol{\theta}}_{k+H} = \widehat{\boldsymbol{\theta}}_{k+H-1} + \boldsymbol{\beta}_{k+H}\left(x_{k+H} - \boldsymbol{c}_{k+\mathrm{H}}\widehat{\boldsymbol{\theta}}_{k+H-1}\right) \tag{14}$$

These values will be then used to perform the downdating operation by removing the sample $(\boldsymbol{c}_k, x_k)$. It is expressed as follows:

$$\underline{A}_{k+H-1} = A_{k+H-1} - \frac{A_{k+H-1}\boldsymbol{c}_{k+\mathrm{H}}^T \boldsymbol{c}_{k+\mathrm{H}} A_{k+H-1}}{1 + \boldsymbol{c}_{k+\mathrm{H}} A_{k+H-1} \boldsymbol{c}_{k+\mathrm{H}}^T} \tag{15}$$

$$\underline{\boldsymbol{\beta}}_{k+\mathrm{H}-1} = \frac{\underline{A}_{k+H-1}\boldsymbol{c}_k^T}{1 - \boldsymbol{c}_k \underline{A}_{k+H-1} \boldsymbol{c}_k^T} \tag{16}$$

$$\underline{\widehat{\boldsymbol{\theta}}}_{k+\mathrm{H}-1} = \widehat{\boldsymbol{\theta}}_{k+H} - \underline{\boldsymbol{\beta}}_{k+\mathrm{H}-1}\left(x_k - \boldsymbol{c}_k \widehat{\boldsymbol{\theta}}_{k+H}\right) \tag{17}$$

Notice that the window width ($H$) must be chosen in order to ensure the invertibility of the matrix ($C_{k+H-1}^{T} C_{k+H-1}$), which not does represent a difficult issue because the sparsity guarantees that only few number of reference signals are used to estimate the current signal. However, when this matrix is not invertible, QR decomposition might be used to enforce the stability of the proposed recursive algorithm [24].

## 3. DATA COLLECTION AND PREPROCESSING

### 3.1 Data collection

Figure 4 shows the specimen considered in this study, which consists of a steel tube with 6.4 m length. It was placed in laboratory conditions where temperature fluctuates between 19°C and 26°C during the monitoring period. This variation is due to the weather changes. The considered tube was used for simultaneous different studies. A first study deals with the behaviour of mechanical guided waves propagation in pipes repaired locally by composite patches [27,28]. This composite repair which is visible on the photo of Figure 4 was deposited on the surface of the pipe to simulate stopping an external corrosion damage. In the present study, another damage, in the same zone, but inside the tube was also machined. This damage mimics a corrosion process.

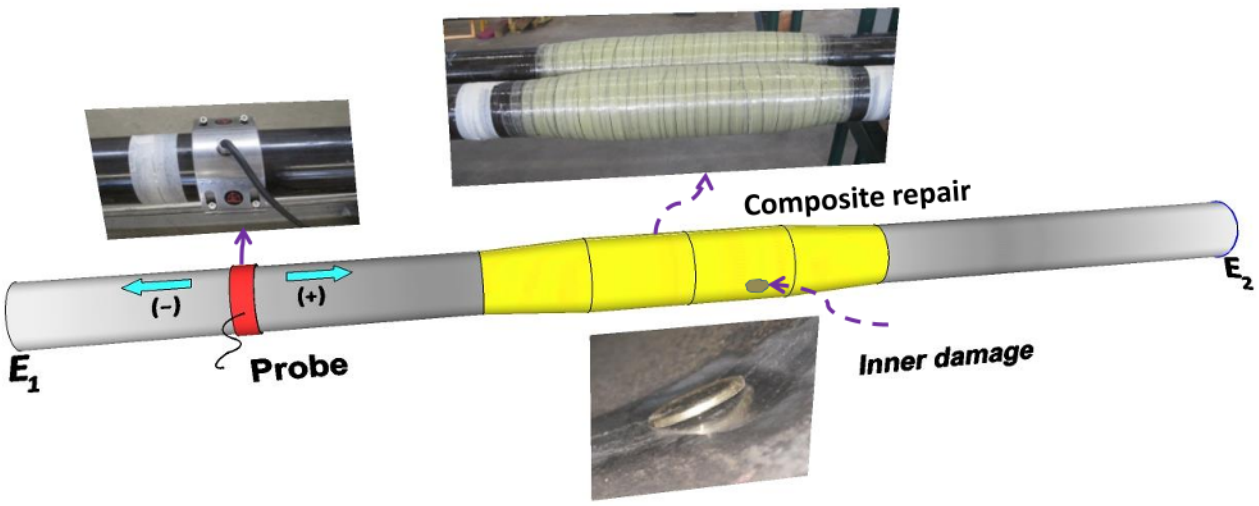


**Figure 4.** Pipeline configuration showing the used sensor, the created damage and the composite repair.

It must be noted that these studies being conducted simultaneously, the detection and the localization of the inner damage is a challenging task as it is known that the composite layers attenuate drastically the UGW.

A probe was placed on the tube as shown in Figure 4. This probe was installed permanently on the surface of the tube (i.e. at least during the period of monitoring study). It acts as an emitter and receiver at the same time (such an arrangement is called pulse-echo). In tubular structures (pipeline in the current study), three types of propagation modes of UGW can coexist: Longitudinal L, Torsional T and Flexural F [29]. Each mode propagates with a specific phase and group velocity. These velocities are generally dependant of the frequency, which confer to the UGW the nature of being dispersive. The used probe allows operating with two separate guided waves modes, which are T (non-dispersive mode) and F (dispersive mode), at five different central frequencies: 14, 18, 24, 30 and 37 kHz. The specimen was monitored during a period around three months. Each week, multiple measurements were scheduled. At each measurement, five signals were acquired in the morning and at the evening in order to capture temperature changes during the day and to investigate its effect on the collected signals. An example of an acquired signal is shown in Figure 5.

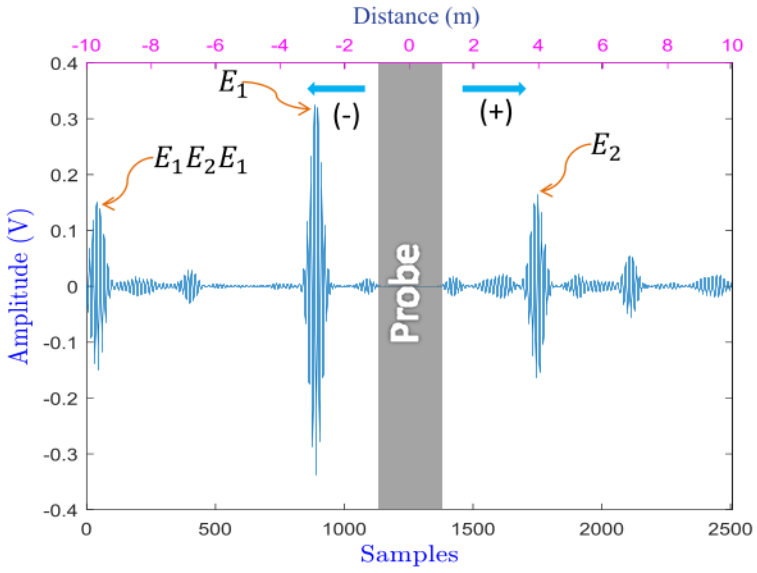


**Figure 5.** Example of an ultrasonic guided wave signal excited with torsional mode (frequency: 14 kHz).

As it can be seen in Figure 5, the middle part of the signal was drawn because it represents the dead zone area (i.e. excitation signal) and the near field. During the former, the acquisition system cannot take acquisition, and during the later, the received echoes don't have the right magnitude, as it should be. Also, a second x axis is shown in the top of this figure, it represents the distance travelled by the UGW in the structure. Actually, time domain is automatically converted into distance domain by the acquisition system, through the velocity of the T(0,1) mode in non-dispersive medium, which is 3200 m/s.

The generated mode, in the current study, is the T(0,1) which is not dispersive since the pipe is empty, and not surrounding by any material. However, when interacting with the repaired zone, some dispersion may occur due to the variation of thickness [30]. This is not observed in the current study, as it can be remarked in Figure 6 which shows a joint time-frequency representation of the received signal. Consequently, no compensation method of the dispersion is required.

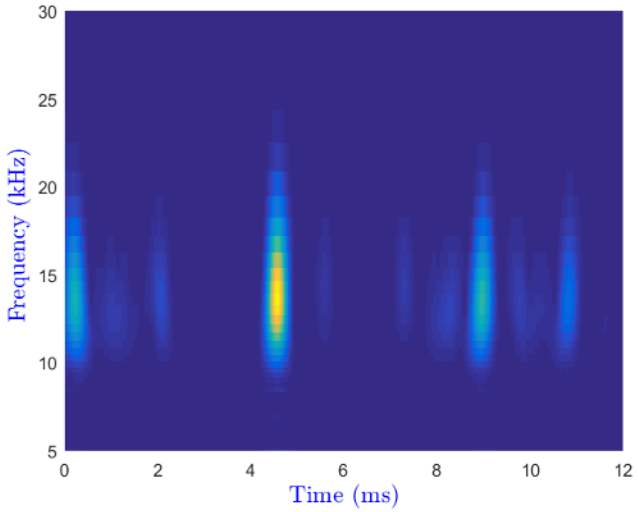


Figure 6: Typical time frequency diagram showing no dispersion of the received signals.

The three echoes with the highest amplitude ($E_1$, $E_2$ and $E_1E_2E_1$), shown in Figure 5, represent multiple reflections from the end of the pipe. Figure 7 gives an explanation of the traveling patch of each one of these echoes. The echoes $E_1$ and $E_2$ correspond to a direct reflection of the UGW by the end of pipe E1 and E2 respectively. While the echo $E_1E_2E_1$ is resulted from a reflection from the end

of pipe E2 and two reflections from the end of pipe E1 as it is shown in Figure 7. The first reflection was received by the sensor which corresponds to the echo $E_1$ but the second reflection produced by the end of pipe E2 was not recorded by the sensor because it was coming from the right direction (+) while the UGW in this case was generated in the left direction (-).

All these echoes have to be removed from the original signal because they can mask small changes induced by the damage. Indeed, the echoes corresponding to damage are too small comparatively to those generated by the geometrical reflectors. It is worth noting that this operation doesn't impact the *in-situ* reliability of the damage detectability. This is because the reflectors are known in advance thanks to the isometric plan of the pipe.

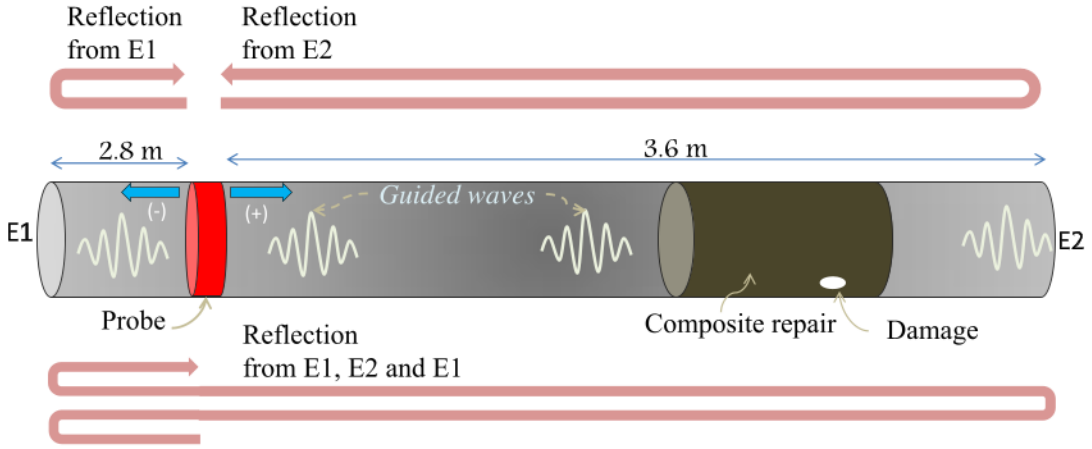


**Figure 7.** Traveling path of the echoes $E_1$, $E_2$ and $E_1E_2E_1$ shown in Figure 4 (not scaled figure).

Damage was created by removing material from the inside of the pipeline in six increasing steps in order to simulate corrosion growing within the structure. Figure 4 (bottom right) shows the defect in the last step (the 1€ coin is shown to have an idea about the size of the damage). The dimensions and the form of this damage were set randomly as in the case of real corrosion, which occurs in real world.

At the end of the monitoring period, a total of 236 signals were collected where 207 ones were collected from the undamaged pipe and 29 signals were acquired from the damaged pipe. Table 1 summarizes information related to the collected database.

**Table 1.** Characteristics of the collected data

| | |
|---|---|
| **Monitoring period** | 3 months |
| **Reference state** | 207 signals |
| **Damage state** | Damage increased in 6 steps (29 signals) |
| **Temperature** | 19 °C → 26 °C |

### 3.2 Temperature effect

The effects of EOCs are a concern of a number of researchers in the SHM community [6,31,32]. The EOCs can affect the amplitude and/or the phase of the recorded signals. Temperature variation includes both effects, as shown in previous studies [10-11]. For this raison and for cost and practicality raisons, temperature is the most investigated factor in the literature [33–35]. In the current study, temperature variation is the main factor that should undergo an influence on the collected signals, since the pipe was installed in a workshop laboratory. The 7°C of temperature variation will have an influence on both amplitude and phase, as demonstrate the results presented in Figure 8. For illustration, two reference signals acquired at different temperatures were served to extract the presented results. For the ease of the reader (i.e. to clearly see the differences between the two signals), a zoom was displayed around the location of the damage (Figure 8 (a)). Figure 8 (b) and (c) show the amplitude and the phase of the Fourier transform, respectively. A significant change in amplitude and phase and also in frequency bandwidth can be easily remarked.

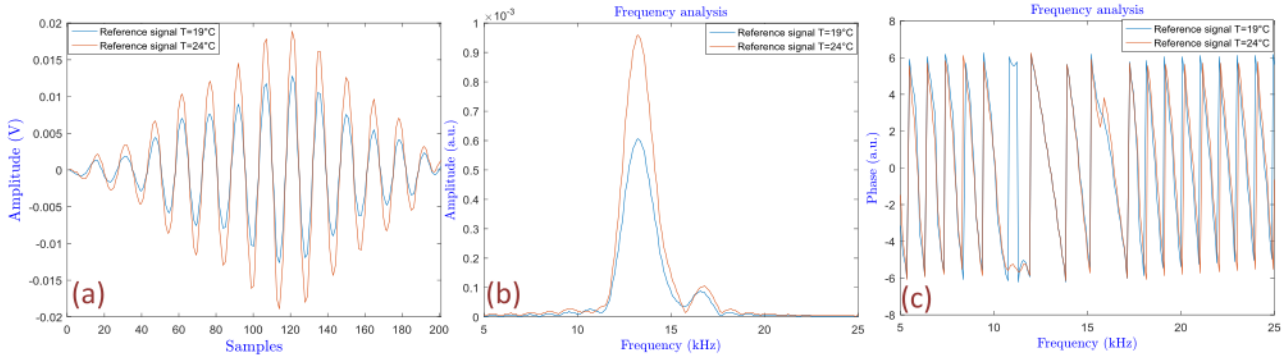


**Figure 8.** Reference signals acquired at different temperatures: waveform (a), spectrum (b), phase (c).

### 3.3 Damage effect

For the purpose of showing the effect of the intentionally created damage on the collected data, two signals were arbitrary chosen (one from the healthy pipe and the other one from the damaged pipe) to be compared. As done in the previous section (3.2), a zoom of the waveform around the damage is shown. The corresponding result is presented in Figure 9 (a). The spectrum and the phase are calculated via Fourier transform, applied on these portions of signals. The obtained results are depicted in Figure 9 (b) and (c), respectively. These results confirm the expected effects of the damage, where just as temperature, there is an impact on the amplitude, the phase as well as the frequency content.

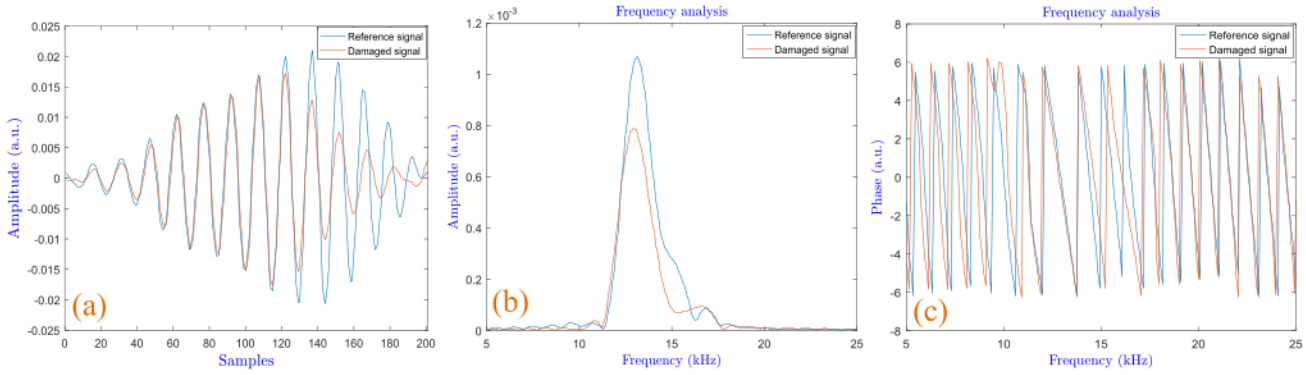


**Figure 9.** Reference signal and a signal from the damaged pipe: waveform (a), spectrum (b), phase (c).

The question that can be asked at this stage is: Is the damage detectable? The answer is surely no! In this case, damage cannot be detected by visual analysis neither in time domain nor in another domain such as frequency one, and this is because the quasi-similarity with the influence of temperature. In another words, without any *a priori* on the nature of the collected signals, it is hard, perhaps even impossible, to distinguish between the effects of EOC (temperature in the present case) and damage. In simple words, one will not be able to confirm that a change in the signals is due to temperature variation or due to the presence of damage. Consequently, the damage cannot be detected. Statistical methods can be envisaged, but the "classical" use of statistical descriptors such as root mean square (RMS), correlation coefficient, standard deviation and maximum

amplitude, as proposed in references [36–38] will not help to detecting damages (in the current database). To illustrate this, let us consider for example the RMS as a damage indicator. As a reminder, the RMS of a signal $\boldsymbol{x} = \{x_i\}$ , $\boldsymbol{x} \in \mathbb{R}^m$ is given by:

$$\mathrm{RMS}(\boldsymbol{x}) = \sqrt{\frac{1}{m}\sum_{i=1}^{m} {x_i}^2} \,. \qquad (18)$$

Figure 10 shows the values of RMS for all monitoring signals (including those from the healthy pipe and the damaged pipe). As it can be seen in this figure, a change of variability (variation between minimum and maximum) in RMS values can be observed between the signals from the undamaged pipe and the signals from the damaged pipe, which indicates that an abnormality has occurred. However, in this case, threshold-based damage detection methods (see for example reference [39]) cannot be used to ensure automatically damage detection. Indeed, any gap cannot be observed between the two types of the pipe state signals (healthy and damaged). Note also that in real world, only one descriptor of the current signal (or a tiny if persistency is considered), is/are to be compared to the baseline database (i.e. healthy state). In this case, the abnormality behaviour that is remarked in Figure 10 cannot be exploited in order to detect damage. Even when considering persistency item, the variability of the few descriptors that should be taken into account in the database of the damaged state of the pipe is quasi-similar to the variability of each five signals collected at each period for repeatability concerns (see zoom in Figure 10 left), and it is too weak in front of the variability of the whole healthy database.

To face this problem, the authors had proposed a damage detection method based on the correction of the collected signals [40]. However, it was found that this method has very low damage sensitivity (that's to say it is not sensitive to small damages). Hence, it is not suitable for the monitoring of pipeline since the main aim of SHM techniques is detecting the initiation of the damage (i.e. defects at early stages). The proposed method for damage detection described in section 2.2, ensures relatively high damage sensitivity. The obtained results using this method are

presented in the next section. In addition, the proposed method allows locating damages, as it will be discovered in section 4.3.

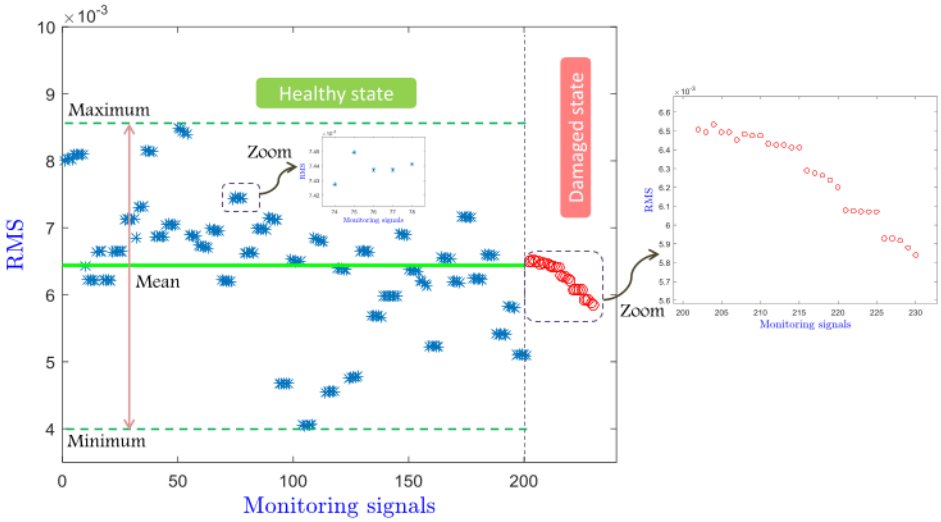


**Figure 10.** RMS of the monitoring signals, the signals from the damaged pipe are coloured in red with a circle marker.

## 4. RESULTS AND DISCUSSIONS

### 4.1 Verification of the condition of using NNLS

One hundred and forty signals were used as a database of reference signals (i.e. matrix $C$) and the others served for the test of the proposed method (as described earlier in Figure 3). The reference signals used for the test step could have been obtained with different variation of temperature, which might not be included in the matrix $C$. Each new signal ($\boldsymbol{x}$) is estimated by sparse model $\widehat{\boldsymbol{\theta}}$ obtained by solving the constrained minimization problem described in equation (5). Here, the sparse estimation is calculated on the entire signal. Let us first verify that the reference signals are positively correlated, which is the condition of using NNLS rather than the non-negative lasso. In this study, the minimum of the covariance matrix was calculated for the reference signals. It is equal to 0.0414, which is of course strictly positive. Thus, the condition of positively correlated signals is fulfilled as stated in inequality (4). To confirm this, Principal Component Analysis (PCA) was firstly performed on the matrix $C$ [41]. Note that at this stage, only torsional mode signals with

an excitation frequency of 14 kHz are considered. Afterthat, the correlation coefficient between the first two representative principal components and the reference signals was calculated. The result is presented in Figure 11.

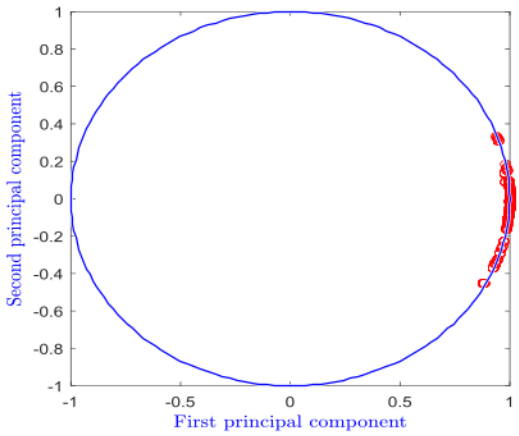


**Figure 11.** Correlation coefficient of the reference signals and the first two principal components.

This result represents the classical correlation circle for the first factorial plane when deploying a Principal Component Analysis on the matrix $C$ containing the reference signals. This figure shows that the reference signals are well represented by the first principal component (the correlation coefficient exceeds 0.88). This can be explained by the fact that there is a strong positive correlation between the reference signals. In this case, the use of NNLS will automatically imply sparsity (i.e. when estimating a signal, the number of selected endogenous signals in the reference database will be limited). The variation of the correlation between the reference signals and the second principal component is probably due to the changes in EOCs namely temperature.

### 4.2 Damage detection

Since the condition of positively correlated signals is now fulfilled, an estimation of a new measured signal can be provided using NNLS. Figure 12 shows the estimation error for a signal from the undamaged pipe (left) and a signal from the damaged pipe (right). It was obtained by subtracting the measured signal with its estimation calculated using NNLS. It can be noticed that the order of magnitude of the estimation error for the signal from the damaged pipe is far from that of the signal from the undamaged pipe. Besides, the estimation error of the undamaged pipe's signal presents a

random behaviour, except in the zones where the echoes from the end of pipe and excitation signal were deleted. When a defect is present, the error will tend to deviate from the random behaviour to a deterministic one. Also, a signal from the damaged pipe will be badly estimated by the reference signals, that's why its estimation error is very high.

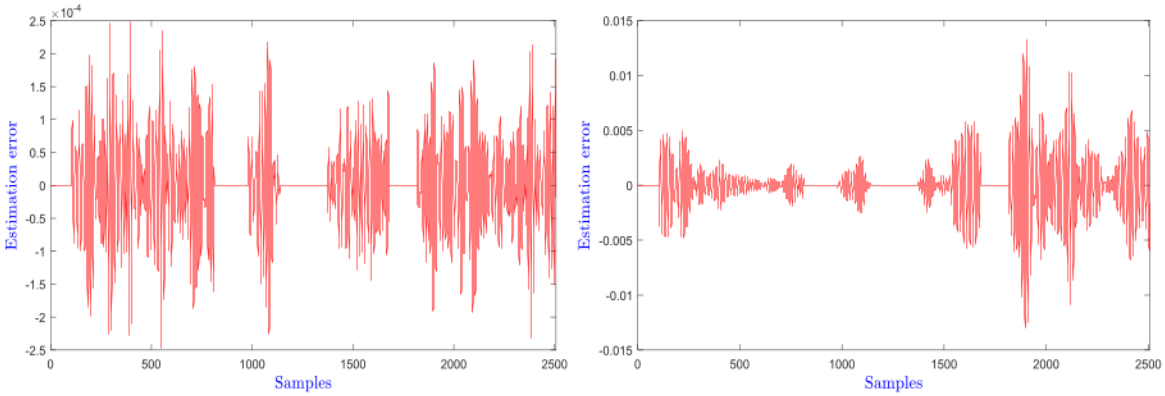


**Figure 12.** Estimation error: reference signal (left), signal from the damaged pipe (right)

The quadratic estimation error $J(\hat{\boldsymbol{\theta}})$ was calculated for all test signals including those from the healthy pipe and the damaged pipe. The flexural mode signals are also considered here for the purpose of comparison. The result is shown in Figure 13.

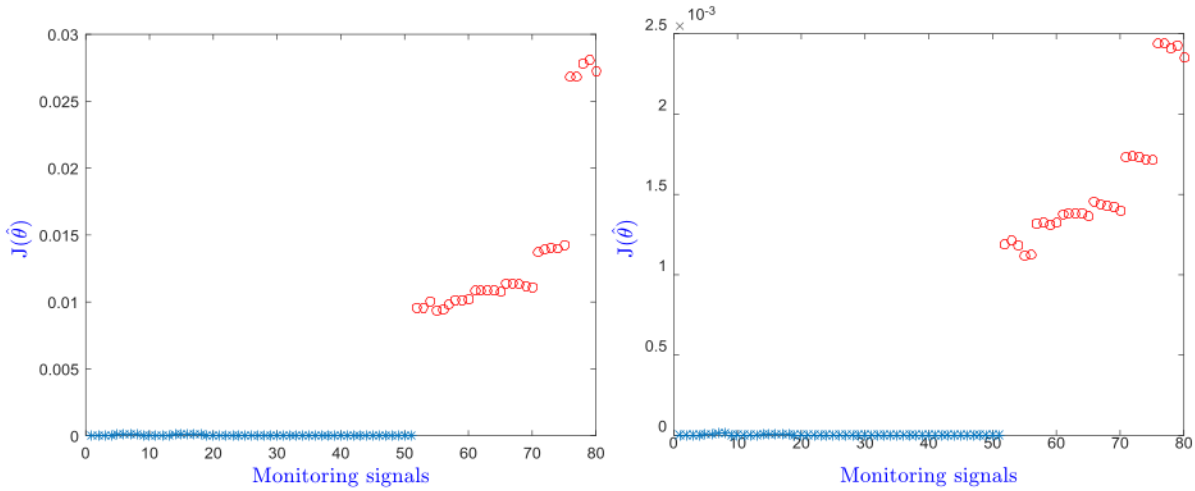


**Figure 13.** Quadratic estimation error $J(\hat{\theta})$ for two different modes (torsional mode: left and flexural mode: right).

Different comments can be drawn from this result:

- Signals from the damaged pipe are well separated from the undamaged pipe's signals for both modes of excitation: torsional or flexural. In this case, damage can be detected

automatically by defining a threshold. Besides, this separation is more significant in the case of flexural mode. This directly affects the damage sensitivity.

- The quadratic estimation error $J(\hat{\theta})$ of the reference signals presents very low variation by comparison to the result of RMS, shown in Figure 10 .
- The values of $J(\widehat{\boldsymbol{\theta}})$ increase as the size of damage increases. Thus, $J(\widehat{\boldsymbol{\theta}})$ can be used to assess the severity of damage.

The sparsity ratio (Sr) defined in equation (10) can be also used to detect a damage. Figure 14 shows the Sr for the monitoring signals including damaged and reference state signals for both excitation modes (i.e. flexural and torsional). The variation of the Sr for the reference signals is somewhat large while the Sr of damaged state signals presents a relatively low variation. Besides, the values of Sr increase as the size of damage increases. However, a threshold cannot be defined to ensure automatic damage detection without triggering false alarms. Thus, $J(\hat{\theta})$ outperforms Sr in terms of damage detectability. In this case, the use of a bivariate indicator, which was defined in equation (11) will be useless. The quadratic estimation error $J(\hat{\theta})$ is sufficient to ensure reliable damage detection.

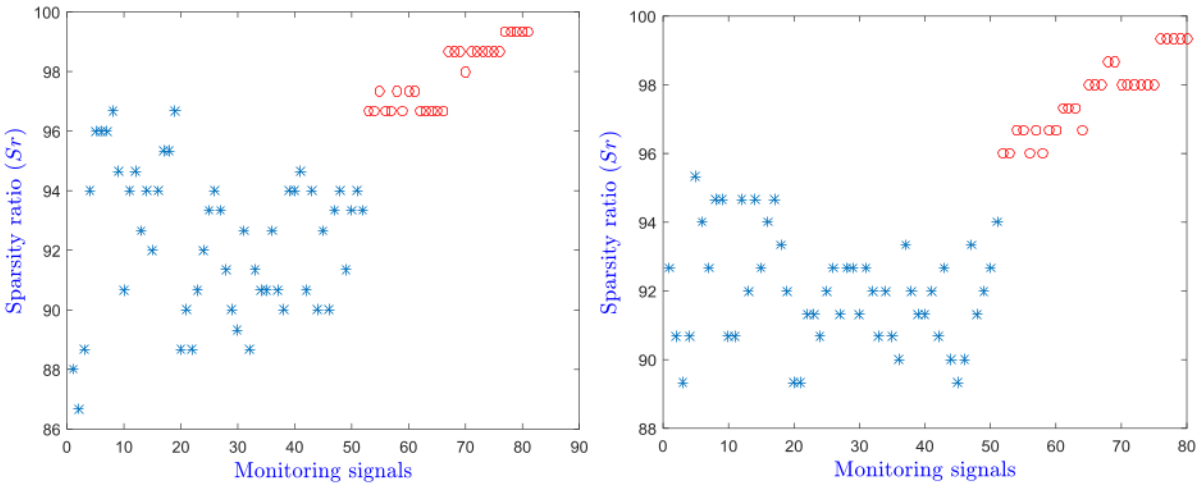


**Figure 14.** Sparsity ratio ***Sr*** of signals from the undamaged pipe and the damaged pipe (torsional mode: left and flexural mode: right).

As mentioned in section 3.1, the acquisition system can excite five different frequencies (14, 18, 24, 30 and 37 kHz). Therefore, the already developed method for damage detection should be applied to all available frequencies in order to select the optimal one to be used in this context. Demma et al [42] have studied the effects of damage size on the reflection of guided waves and have concluded that the maximum amplitude of the reflected wave from a defect can be noticed when using a wide range of frequency. The results showed in Figure 15 confirmed that the excitation frequency severely impacts the damage sensitivity because when the frequency increases the damage sensitivity decreases.

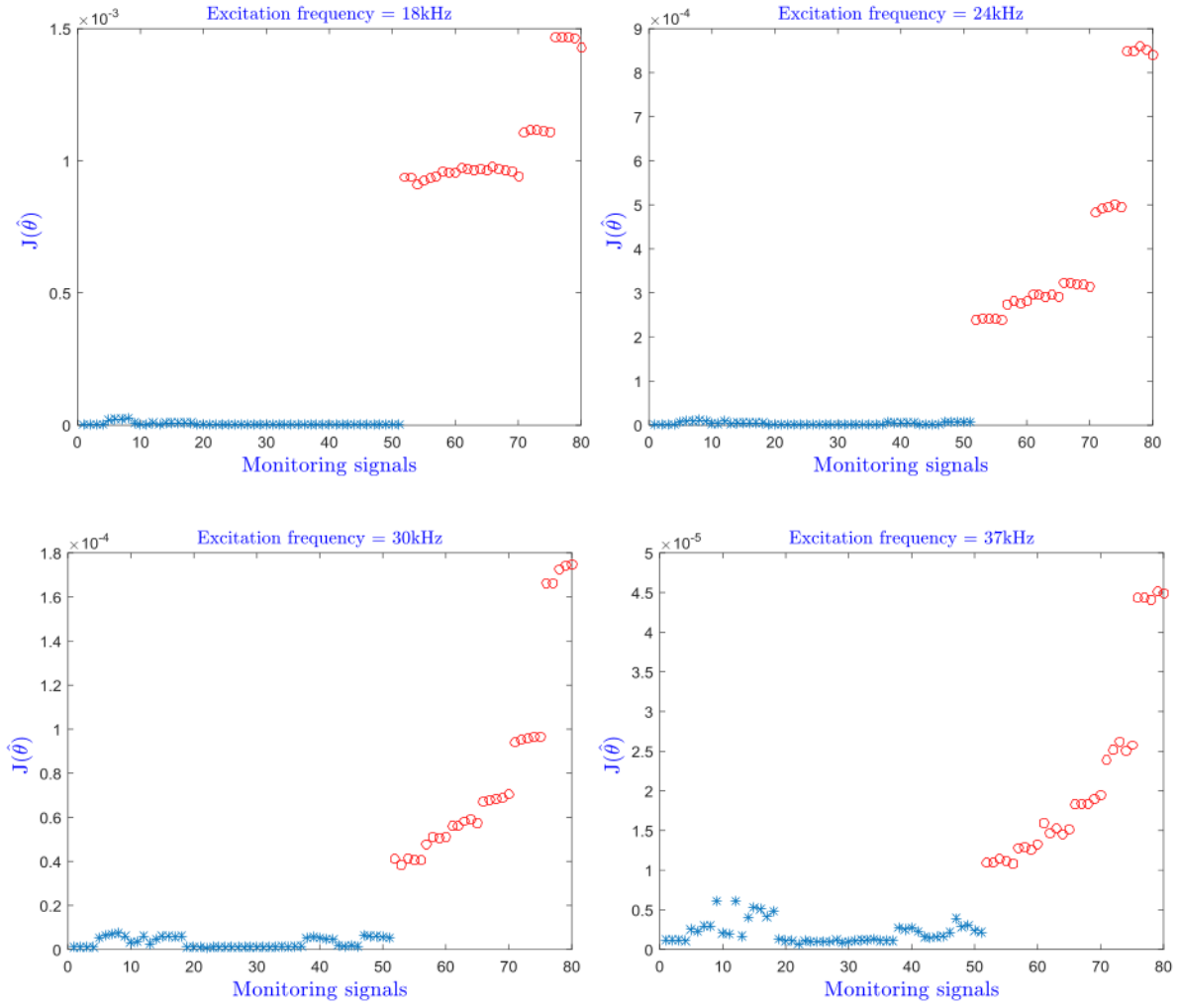


**Figure 15.** Frequency effect on damage detectability for flexural propagation mode.

To illustrate this, a ratio which quantifies the gap between reference signals and damaged state signals was calculated for all acquired signals at different excitation frequencies and for both modes of propagation. This ratio can be expressed as:

$$Gr = \frac{\mathrm{J}(\widehat{\boldsymbol{\theta}})\ [\text{first damaged pipe's signal}]}{\mathrm{J}(\widehat{\boldsymbol{\theta}})\ [\text{last undamged pipe'ssignal}]} \qquad (19)$$

The results are reported in table 2. In overall, flexural mode ensures high damage sensitivity compared to torsional mode. This might be explained by the fact that the dispersive nature of the flexural mode emphasizes the interaction between damage and the guided waves. Thus, damage effect is more significant in this case.

**Table 2.** Gap ratio (Gr) between reference signals and damaged state signals (following eq. 19)

| Frequency / Mode | 14 kHz | 18 kHz | 24 kHz | 30 kHz | 37 kHz |
|---|---|---|---|---|---|
| Torsional | 582 | 280 | 19 | 6 | 2 |
| Flexural | **978** | 732 | 30 | 8 | 5 |

### 4.3 Axial damage localization

To locate the damage through the axes of pipe revolution (i.e. one dimensional localization), the idea which was described in section 2.4, is to apply the sparse estimation on a sliding window over the signal (i.e. samples) as shown in Figure 16. As it has been mentioned in the introduction, when UGW are excited by the sensor, they travel in all directions. At the position of damage, they interact with it and the echo resulted from this interaction travel back to the sensor. By analysing the received signal, a significant change must be observed at the position of damage. Hence, the local comparison between reference signals and damaged state signal is ensured by considering a window which moves over the damaged pipe's signal. At each step, we measure how different is this portion of the signal from the same portion in the references signals. This is done by calculating the quadratic estimation error using NNLS. Finally, the position of damage is characterized by a

very high quadratic estimation error. In this case, the window width may influence the final result. It can be determined basing on the desired precision of localization. It has to be noted that, the problem here is not to localize precisely the position of damage as in the case of imaging method but only to give an estimation of the distance that separate the sensor to the defect.

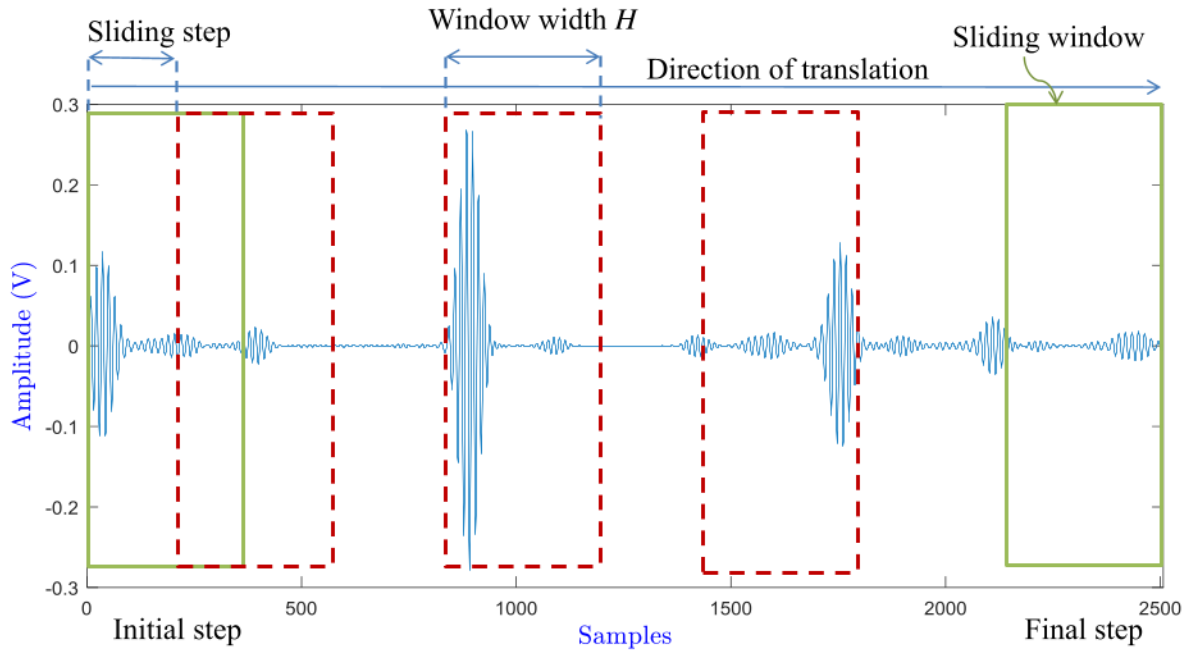


**Figure 16.** Sliding window over a signal from the damaged pipe.

In the present study, the window width was set at forty samples. A larger window width could be tested to investigate its influence on the result of localization. This window was moved with one sample per step. At each step, the quadratic estimation error $J(\hat{\boldsymbol{\theta}})$ using recursive NNLS algorithm is calculated. At the end, at each moving window over the signal from the damaged pipe, a value of $J(\hat{\boldsymbol{\theta}})$ is obtained.

As it can be seen in Figure 17, the position of the machined defect is found for both modes (flexural and torsional). To avoid interpretation of false damage position, the signal from the damaged pipe was truncated between the first two arrivals of the end of pipe echoes. This figure shows that the position of damage, which corresponds to the maximum of $J(\hat{\boldsymbol{\theta}})$, is 3 m for torsional mode and 2.8 m for flexural mode. The real position of damage is 2.6 m. Hence, the flexural mode is more precise

in terms of damage localization. The error of localization is 15% and 7% for torsional and flexural modes, respectively. It can be explained by the fact that the window width ($H$) induces an error of localization. Finally, it is worth noting that the result of localisation could be optimized by assigning the position of damage to a value of $J(\hat{\boldsymbol{\theta}})$ where we estimate that the error is significant and not necessarily to the maximum of $J(\hat{\boldsymbol{\theta}})$.

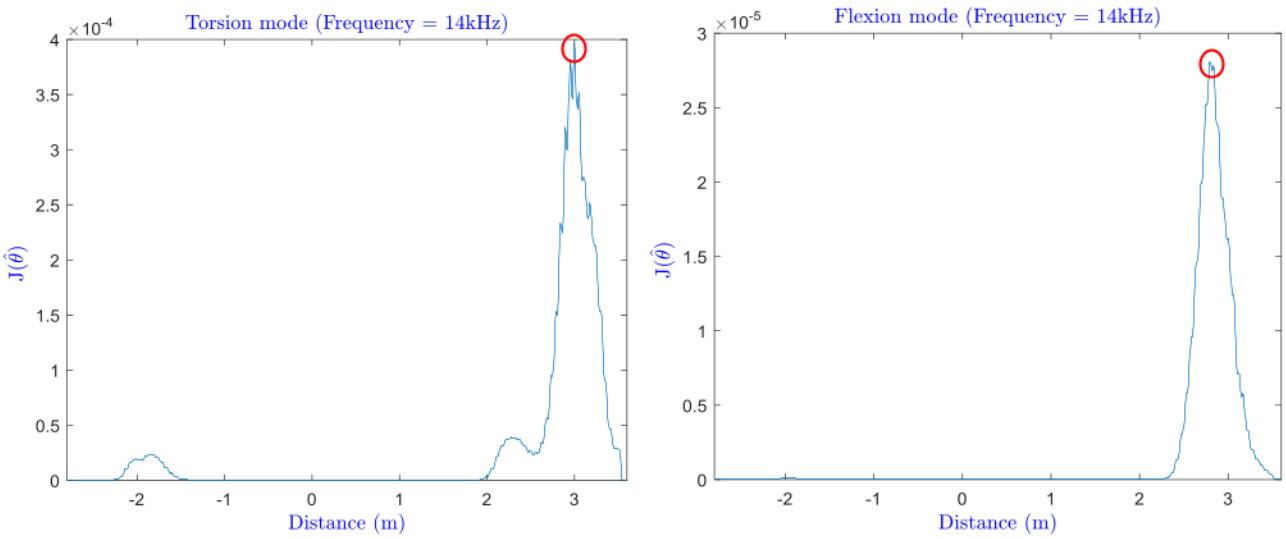


**Figure 17.** Quadratic estimation error $J(\hat{\boldsymbol{\theta}})$ of a signal from the damaged pipe showing the position damage (left: torsional mode and right: flexural mode).

## 5. CONCLUSION

In this paper, a method for damage detection and localization in pipeline was proposed. It is based on sparse estimation of the current signals by the reference signals. A simplified form of this estimation using the non-negative least squares was investigated. It is based on the fact that the acquired UGW signals are highly correlated. The sparsity helps to enhance damage detectability because a signal from the damaged pipe will have a high estimation error compared to that of a signal from the undamaged pipe. Besides, it can face the problem of variation in EOCs provided that the database of reference signals contains large variations of these EOCs. The detection of the damage was ensured by calculating the quadratic estimation error $J(\hat{\boldsymbol{\theta}})$ on the entire current signal. The localization of the damage was established however through implementing a recursive

version of the sparse estimation on a sliding window over the signal from the damaged pipe. It was shown that the flexural mode provides better damage sensitivity and better precision of damage localization.

As a perspective of this work, an update of the database of reference signals could be considered in the case where these signals present limited variation in EOCs. This can be achieved by adding to this database, new signals from the undamaged pipe with unknown variation in EOCs. Also, the proposed method has to be validated on operational pipeline, which serves in different EOCs.

## ACKNOWLEGMENT

This work is a part of Hydrogen Horizon Energy (H2E) project, which is supported in part by BpiFrance foundation. The authors would like to thank their partners, more particularly STELIA Composites and Air Liquide for their collaboration. The authors are also grateful for the Association Nationale Recherche Technologie for the partly financial support of M. El Mountassir's PhD thesis through the CIFRE convention.

## REFERENCES

[1] C.R. Farrar, K. Worden, An introduction to structural health monitoring., Philos. Trans. A. Math. Phys. Eng. Sci. 365 (2007) 303–15.

[2] K. Worden, C.R. Farrar, G. Manson, G. Park, The fundamental axioms of structural health monitoring, Proc. R. Soc. A Math. Phys. Eng. Sci. 463 (2007) 1639–1664.

[3] A. Galvagni, Pipeline health monitoring, Thesis submitted to Imperial College of London (2013).

[4] J.L. Rose, Ultrasonic guided waves in solid media. Cambridge University Press, (2014).

[5] M.J.S. Lowe, D.N. Alleyne, P. Cawley, Defect detection in pipes using guided waves, Ultrasonics. 36 (1998) 147–154.

[6] H. Sohn, Effects of environmental and operational variability on structural health monitoring, Philos. Trans. A. Math. Phys. Eng. Sci. 365 (2007) 539–60.

[7] J. Kullaa, Statistical analysis of the damage detection performance under environmental or operational influences. 9th International Conference on Structural Dynamics, EURODYN, Porto, Portugal, 30 June – 2 July 2014.

[8] J. Kullaa, Distinguishing between sensor fault, structural damage, and environmental or operational effects in structural health monitoring, Mech. Syst. Signal Process. 25 (2011) 2976–2989.

[9] T. Clarke, F. Simonetti, P. Cawley, Guided wave health monitoring of complex structures by sparse array systems: Influence of temperature changes on performance, J. Sound Vib. 329 (2010) 2306–2322.

[10] A. Marzani, S. Salamone, Numerical prediction and experimental verification of temperature effect on plate waves generated and received by piezoceramic sensors, Mech. Syst. Signal Process. 30 (2012) 204–217.

[11] S. Ha, K. Lonkar, A. Mittal, F.K. Chang, Adhesive Layer Effects on PZT-induced Lamb Waves at Elevated Temperatures, Struct. Heal. Monit. 9 (2010) 247–256.

[12] Rizzo P, Lanza di Scalea F. Wavelet-based unsupervised and supervised learning algorithms for ultrasonic structural monitoring of waveguides. Progress in Smart Materials and Structures Research. Nova Science Publishers: Hauppauge, NY. (2006), Chapter 8.

[13] C. Liu, J.B. Harley, M. Bergés, D.W. Greve, I.J. Oppenheim, Robust ultrasonic damage detection under complex environmental conditions using singular value decomposition, Ultrasonics. 58 (2015) 75–86.

[14] M. Eybpoosh, M. Bergés, H. Y. Noh, Sparse representation of ultrasonic guided waves for robust damage detection in pipelines under varying environmental and operational conditions. Journal of Structural Control and Health Monitoring. 23 (2016) 369-391.

[15] R. Tibshirani, Regression Shrinkage and Selection via the Lasso, J. R. Stat. Soc. Ser. B Stat. Methodol. 58 (2007) 267–288.

[16] N. Meinshausen, Sign-constrained least squares estimation for high-dimensional regression, Electron. J. Stat. 7 (2013) 1607–1631.

[17] M. Slawski, M. Hein, Non-negative least squares for high-dimensional linear models: Consistency and sparse recovery without regularization, Electron. J. Stat. 7 (2013) 3004–3056.

[18] D. P. Bertsekas, Nonlinear programming. Belmont : Athena scientific, (1999).

[19] D. Chen, R. J. Plemmons, Nonnegativity constraints in numerical analysis, In The birth of numerical analysis. (2010) 109-139.

[20] C. L. Lawson, R. J. Hanson, Solving least squares problems, Society for Industrial and Applied Mathematics, 1995.

[21] M. Eybpoosh, M. Berges, H.Y. Noh, An energy-based sparse representation of ultrasonic guided-waves for online damage detection of pipelines under varying environmental and operational conditions, Mech. Syst. Signal Process. 82 (2017) 260–278.

[22] G. Boracchi, D. Carrera, B. Wohlberg, Novelty detection in images by sparse representations, IEEE Symposium on Intelligent Embedded Systems (IES), Orlando, FL, USA, 9–12 December 2014.

[23] R. A. Johnson, D. W. Wichern, Applied multivariate statistical analysis, New Jersey: Prentice-Hall. (2014).

[24] Å. Björck, Numerical methods for least squares problems, Society for Industrial and Applied Mathematics. (1996).

[25] A. Mosesov, Adaptive Non-negative Least Squares with Applications to Non-Negative Matrix Factorization, Master dissertation, University of Minnesota. (2014).

[26] Q. Zhang, Some Implementation Aspects of Sliding Window Least Squares Algorithms, 12th IFAC Symposiun on Systems identification, SYSID 2000, Santa Barbara, CA, USA, 21-23 June 2000.

[27] S. Yaacoubi, W. Ke, F. Dahmene, M. El Mountassir, Investigations of mechanical guided waves propagation in pipes repaired locally by composite patches, European Congress on Computational Methods in Applied Sciences and Engineering (ECCOMAS), Crete Island, Greece, 5-10 June 2016.

[28] S. Yaacoubi, M.E. Mountassir, F. Dahmene, Guided Waves for the monitoring of pipeline zones under composite repairs: From comprehensive to pre-deployment investigations, 8th European Workshop on Structural Health Monitoring (EWSHM), Bilbao, Spain, 5-8 July 2016.

[29] S. Izadpanah, G. Rashed, S. Sodagar, Using ultrasonic guided waves in evaluation of pipes, 2nd International Conference on technical inspection and NDT, Tehran, Iran, October 2008.

[30] F. Simonetti, Sound Propagation in lossless Waveguides coated with attenuative. Thesis submitted to Imperial College of London (2003).

[31] J.E. Michaels, S.J. Lee, T.E. Michaels, Impact of applied loads on guided wave structural health monitoring, AIP Conf. Proc. 1335 (2011) 1515–1522.

[32] M. Eybpoosh, M. Bergés, H. Y. Noh, Investigation on the effects of environmental and operational conditions (EOC) on diffuse-field ultrasonic guided-waves in pipes. In Computing in Civil and Building Engineering (2014) 1198-1205.

[33] R.L. Weaver, O.I. Lobkis, Temperature dependence of diffuse field phase, Ultrasonics. 38 (2000) 491–494.

[34] A. Raghavan, C.E.S. Cesnik, Effects of Elevated Temperature on Guided-wave Structural Health Monitoring, J. Intell. Mater. Syst. Struct. 19 (2008) 1383–1398.

[35] Y. Lu, J.E. Michaels, A methodology for structural health monitoring with diffuse ultrasonic waves in the presence of temperature variations, Ultrasonics. 43 (2005) 717–31.

[36] P. Rizzo, Feature Extraction for Defect Detection in Strands by Guided Ultrasonic Waves, Struct. Heal. Monit. 5 (2006) 297–308.

[37] M. Radzieński, L. Doliński, M. Krawczuk, A. Zak, W. Ostachowicz, Application of RMS for damage detection by guided elastic waves, J. Phys. Conf. Ser. 305 (2011).

[38] J.E. Michaels, T.E. Michaels, Ultrasonic signal processing for structural health monitoring, Rev. Quant. Nondestruct. Eval. 23 (2004) 1476–1483.

[39] P. Rizzo, E. Sorrivi, F. Lanza di Scalea, E. Viola, Wavelet-based outlier analysis for guided wave structural monitoring: Application to multi-wire strands, J. Sound Vib. 307 (2007) 52–68.

[40] M.E. Mountassir, S. Yaacoubi, G. Mourot, D. Maquin. Studies on data correction of Structural Health Monitoring using ultrasonic guided waves: case of study. 8th European Workshop on Structural Health Monitoring (EWSHM), Bilbao, Spain, 5-8 July 2016.

[41] I.T. Jolliffe, Principal Component Analysis, Second Edition, Encycl. Stat. Behav. Sci. 30 (2002) 487.

[42] A. Demma, P. Cawley, M. Lowe, A. G. Roosenbrand, B. Pavlakovic, The reflection of guided waves from notches in pipes: A guide for interpreting corrosion measurements, NDT&E Int. 37 (2004) 167–180.